Cardiovasc Intervent Radiol (2019) 42:880–885
https://doi.org/10.1007/s00270-019-02181-1

LABORATORY INVESTIGATION

Does Drug-Eluting Bead TACE Enhance the Local Effect of IRE? Imaging and Histopathological Evaluation in a Porcine Model

Peter Isfort[1] · Philip Rauen[1] · Hong-Sik Na[1] · Nobutake Ito[1] · Saskia von Stillfried[1] · Christiane Kuhl[1] · Philipp Bruners[1]

Received: 7 November 2018 / Accepted: 4 February 2019 / Published online: 8 February 2019

Abstract
Objectives We conducted an in vivo trial on swine to compare the ablation volumes of irreversible electroporation (IRE) followed by drug-eluting beads transarterial chemoembolization (DEB-TACE) versus IRE only.
Materials and Methods Nine swine underwent CT-guided IRE in one liver lobe and IRE immediately followed by DEB-TACE in a different liver lobe. For DEB-TACE, 100–300 µm beads (DC-Beads®) were loaded with 50 mg doxorubicin. For IRE, the NanoKnife® was used employing two electrodes according to the vendor's protocol. Imaging follow-up was performed including CT-based lesion volume assessment using contrast-enhanced CT (venous phase) on days 1, 3, and 7 after the procedure. Three animals were killed for histopathological analysis after each follow-up.
Results Ablation volumes in CT in the IRE + DEB-TACE group were 15.4 ± 10.5 ml on day 1, 8.7 ± 5.6 ml on day 3, and 1.6 ± 0.7 ml on day 7. In the IRE group, the corresponding values were 5.2 ± 5.2 ml on day 1, 1.0 ± 1.2 ml on day 3, and 0.1 ± 0.1 ml on day 7. On day 1 and day 3, ablation volumes of IRE + TACE group were significantly larger than in the IRE group ($p < 0.05$). 96% of beads were depicted in or around ablative lesions. 69% of these beads were found in the surrounding hemorrhagic infiltration and 31% within the ablative lesion itself.
Conclusions Combination of IRE immediately followed by DEB-TACE resulted in larger ablation volumes compared to IRE alone, suggesting that local efficacy of IRE can be enhanced by post-IRE DEB-TACE.

Keywords Irreversible electroporation · Transarterial chemoembolization · Drug-eluting bead TACE · Hepatocellular carcinoma · Experimental study

Introduction

Minimal invasive percutaneous treatment of primary or secondary liver tumors is well established in selected patients. Different local ablative techniques including radiofrequency ablation (RFA), laser-induced thermal therapy (LITT), microwave ablation (MWA), cryoablation (Cryo), and irreversible electroporation (IRE) are available, among which IRE is the latest promising technique. In IRE, short electrical pulses induce irreversible defects to the cell membranes, leading to controlled cell death in the treated region. When compared to other ablative techniques, IRE does not rely on thermocoagulation (either heating or freezing) which offers several advantages: No heat sink or cold sink effects, which typically have a significant impact on the ablation result near larger vessels, have to be taken into account. Furthermore, recent studies suggest safe application of IRE in the vicinity of vulnerable structures like bile ducts or the pancreatic duct [1]. This is the reason

✉ Peter Isfort
Isfort@ukaachen.de

[1] Department of Diagnostic and Interventional Radiology, RWTH Aachen University Hospital, Pauwelsstrasse 30, 52074 Aachen, Germany

why IRE is also applied for local tumor treatment in the pancreas or even in the prostate [2].

Our experience as well as recently published data shows a hyperperfused rim surrounding hepatic tumors immediately after treatment with IRE in contrast-enhanced computed tomography (CECT) [3–5]. On the other hand, corresponding to a decrease in electrical field strength, an area of reversible cell membrane defects, i.e., reversible electroporation is located in the periphery of IRE lesions [1, 6]. However, reversible electroporation itself is a well-established technique in biochemistry to introduce large molecules or even biological vectors into vital cells [7].

In difficult anatomic locations, e.g., hepatic dome next to vena cava and/or liver veins, it can be demanding to achieve a good needle placement in order to obtain a complete ablation. In such cases, the additional effect of a transarterial treatment could be beneficial.

Drug-eluting bead transarterial chemoembolization (DEB-TACE) using doxorubicin-eluting beads is an established technique for the treatment of unresectable hepatocellular carcinoma (HCC). The PRECISION V trial revealed that patients with advanced disease better tolerated DEB-TACE and showed improved imaging responses compared with patients treated with conventional oil-based TACE [8]. In this study, significantly less liver toxicity and less side effects of DEB-TACE compared with conventional TACE were demonstrated in patients with preserved liver function. Even in cases of advanced liver deterioration (Child–Pugh B, ECOG 1, and bilobar or recurrent disease), a significantly better local response has been noted.

With respect to a possible overlap of a hyperperfused rim-like zone surrounding IRE lesions in the liver after the procedure and a zone of reversible electroporation, the aim of our study was to investigate whether additional DEB-TACE of the corresponding liver segment immediately following IRE leads to a selective accumulation of beads and enhances the local efficacy of IRE.

Materials and Methods

Animal Experiments

In nine female domestic pigs (Sus scrofa domesticus) with a mean weight of 64.4 ± 6.8 kg, experiments were performed in accordance with and after allowance by the local regulatory board (Ministry of Environment, Nature and Consumer Protection). All interventions were done under general anesthesia after orotracheal intubation and mechanical ventilation. Additionally, pancuronium was administered for deep muscle relaxation. For the experiments, animals were placed on the CT table in supine position (Siemens Somatom Definition Flash, Siemens Healthcare). For the depiction of the individual liver anatomy and planning of the IRE, a contrast-enhanced CT scan in arterial and venous contrast phase (Ultravist 370, 1,5 ml/kg of body weight, Bayer Healthcare Pharmaceuticals) was performed during expiratory breath hold (collimation: 5 mm, 120 kV, 210 mAs; pitch: 1.0; slice thickness/gap: 5/4 mm and 1/0.7 were reconstructed).

Prior to the intervention, DEB (DC-Beads, 100–300 µm, Biocompatibles Ltd.) was loaded with 50 mg doxorubicin in the standard fashion as recommended. After removal of excessive fluid from beads they were incubated with a 50 mg doxorubicin solution, made from powder mixed with 2 ml sterile water (Adriablastin, Pfizer, New York, USA). After a sufficient incubation time, contrast (Ultravist 300, Bayer Vital GmbH, Leverkusen, Germany) was added.

Under fluoroscopic guidance using a mobile C-arm (Arcadis Orbic 3D, Siemens Healthcare) that was used with the animal placed supine on the CT table, a 5-F catheter (Glidecath, Terumo, Japan) in cobra or sidewinder configuration was placed in the celiac trunk via a 5-F sheath (Radifocus Introducer II, Terumo, Tokyo, Japan), and a 2.7-F microcatheter (Progreat, Terumo) was placed in the desired liver segment artery. Thereafter, a CT in arterial contrast phase with the contrast agent being administered via the microcatheter was acquired to confirm the correct position of the microcatheter. This CT image dataset acted as a planning scan for the placement of the IRE probes. For the IRE, the NanoKnife system (AngioDynamics) with a two-probe setup (NanoKnife single electrode activation probe; NanoKnife single electrode probe; AngioDynamics) was used. The probes were placed in the center of the contrast-enhancing liver segment in a parallel fashion with a distance of 2 cm from each other. Tip exposure was 1.5 cm. IRE was performed with 90 pulses, a pulse length of 90 µs and field strength of 1500 V/cm. Figure 1 illustrates treatment planning and needle placement.

Immediately after completion of ablation, DEB-TACE was performed under fluoroscopic control until stasis was achieved in the treated segmental artery. After a 5-min waiting time, embolization was continued until second stasis was achieved (embolization endpoint). Afterward the microcatheter was removed, and a vascular closure device (AngioSeal VIP, 6F, St. Jude Medical) was applied. Afterward, an IRE employing the same parameters as described above was performed in a different liver lobe without additional DEB-TACE. This procedure served as a control and was performed in a different liver lobe to avoid bias by non-target embolization.

Thereafter, a contrast-enhanced control CT scan was performed using the same parameters as the initial CT.

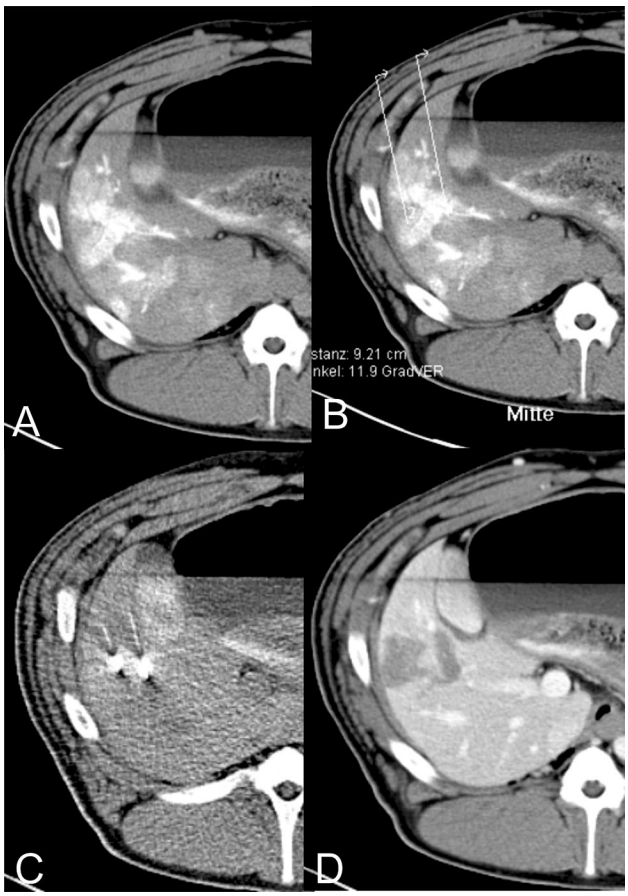

Fig. 1 Approach of IRE needle placement in IRE/DEB-TACE group. **A** CT after transarterial contrast administration via microcatheter. **B** Planning of needle placement. **C** IRE needles in place prior to the procedure. **D** Lesion post-IRE/DEB-TACE

Finally, animals were transferred to the animal research department, and anesthesia was ceased. For follow-up, imaging CT scans were performed using the same protocol as mentioned above.

On the day after the experiment, follow-up imaging was performed in all nine animals. Thereafter, three animals were killed euthanized (acute group). On day 3 after the experiment, identical follow-up, imaging was performed in the six remaining animals; thereafter three further animals were killed euthanized (subacute group). One week after the experiment, final follow-up imaging was performed using the same protocols, after which the remaining three animals were killed euthanized (chronic group). Based on imaging data, volume assessment of the lesions was performed with ROI segmentation (OsiriX 5.8.5, Pixmeo, Bernex, Switzerland) using CT datasets in venous contrast phase. Thereby newly established non-contrast-enhancing foci were counted as ablation zone.

Pathological Evaluation

After completion of the experiments, animals were killed euthanized; livers were harvested and fixed in formalin. Then livers were sliced in 6 mm slice thickness and were analyzed macroscopically. Ablation lesions could be identified in all cases. All slices were documented photographically including a ruler for calibration.

For histologic evaluation, representative slices were stained with hematoxylin–eosin. For the analysis of the bead distribution, a total of 43 slices were analyzed. These slices contained either IRE lesions, IRE + DEB-TACE lesions or slices randomly derived from areas that were left without treatment.

See also Fig. 3 for details on the macroscopic and histologic evaluation.

Statistical Analysis

Statistical analysis was performed using SAS 9.4 (Statistical Analysis System, SAS Institute). Mean and standard deviation were calculated for all lesion volume data. Related t-test was used to compare the groups. In comparisons, $p < 0.05$ was considered significantly different.

Results

All experiments were performed successfully. One animal of the chronic group was excluded from the study because it developed a large liver infarction following DEB-TACE.

Ablation volumes measured in CT imaging in the venous phase in the IRE + TACE group were 15.4 ± 10.5 ml on day 1, 8.7 ± 5.6 ml on day 3, and 1.6 ± 0.7 ml on day 7. In the IRE group, the corresponding values are 5.2 ± 5.2 ml on day 1, 1.0 ± 1.2 ml on day 3, and 0.1 ± 0.1 ml on day 7.

On day 1 and day 3, follow-up CT imaging ablation volumes of IRE + TACE groups were significantly larger than in the IRE groups ($p < 0.05$).

See also Fig. 2 for ablation volumes in follow-up CT imaging.

In pathological evaluation, ablation lesions on the first day after the experiment appeared as areas of necrosis (i.e., white necrosis) with a broad zone of hemorrhagic infiltrations (i.e., red necrosis/sinusoidal congestion) surrounding it. On day 3 after the experiment, hemorrhagic infiltration is partly replaced by areas of fibrosis accompanied by bile duct dilations. In the chronic group, hemorrhagic infiltrations are completely replaced by fibrosis and more pronounced bile duct dilations.

Figure 3 illustrates pathological findings induced by IRE and IRE + TACE.

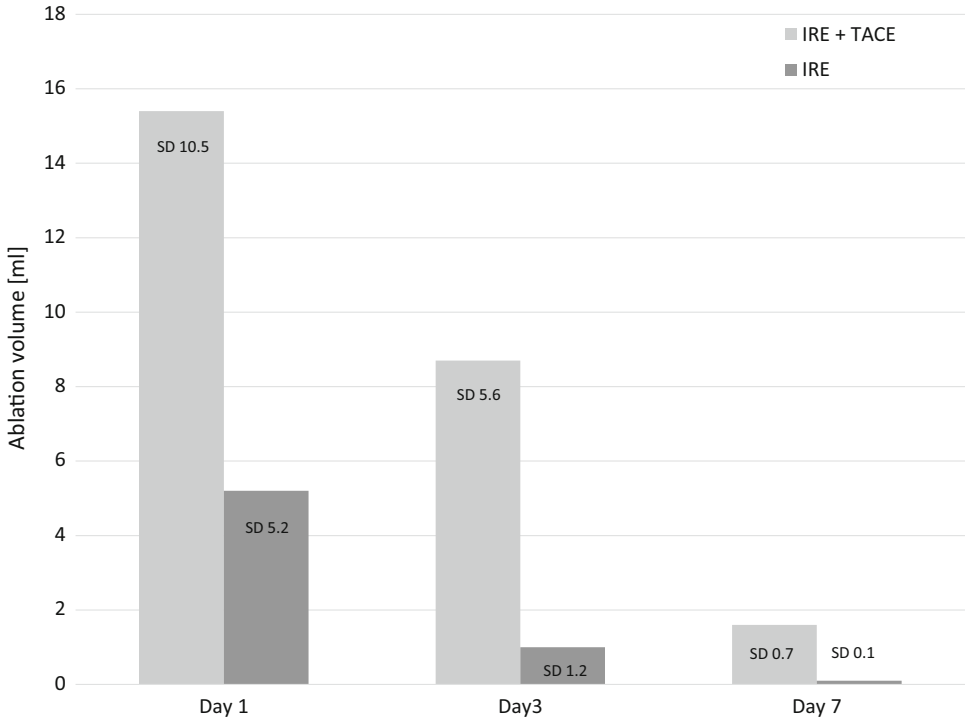

Fig. 2 Mean volume of lesions after IRE and IRE-TACE procedures in follow-up CT imaging

In the analysis of bead distribution, a total of 368 beads were counted. Out of these, 355 (96%) beads were detected in slices obtained from IRE and TACE lesions. Thirteen beads (4%) were found in the surrounding regular liver tissue, representing non-target embolization. In the slices containing IRE + TACE lesions, 244 beads (69%) were detected inside the zone of hemorrhagic infiltration, whereas the remaining 111 beads (31%) were found inside the areas surrounded by the hemorrhagic infiltration, i.e., inside ablation volumes.

Discussion

The combination of transarterial and percutaneous therapies like RFA plus TACE is an established treatment option for large hypervascularized liver tumors resulting in a significant longer overall survival and recurrent-free survival compared to treatment with RFA alone [9]. The sequential use of IRE followed by DEB-TACE loaded with doxorubicin resulted in our in vivo study in significantly larger ablation volumes when compared to IRE alone.

Based on our observations as well as IRE literature, a hyperperfused rim-like area can be observed after IRE especially in the arterial contrast phase [4, 5]. The rationale to perform the combination treatment in the sequence, (1) IRE—(2) DEB-TACE, is based on these findings. Post-therapeutic hyperemia can be used to selectively gather the beads in the target zone as shown by the histopathological analysis. In contrast to other ablation modalities, IRE is not susceptible to a heat sink, so prior devascularization by means of transarterial embolization does not seem to be useful. On the other hand, due to a decrease in the field strength, there is a zone of reversible electroporation surrounding the IRE zone [10]. This means that tumor cells in this area may not be treated sufficiently, possibly resulting in incomplete ablation. Reversible electroporation can be exploited to increase intracellular chemotherapy concentration [11]. So local application of chemotherapeutic agents in the zone of reversible electroporation, e.g., using drug-eluting beads, may lead to an enhanced tumor necrosis because of both a perfusion-mediated accumulation of drug-eluting beads and an enhanced intracellular uptake of chemotherapy—especially in the periphery of IRE lesions, counteracting potential undertreatment with IRE. Nevertheless, there are insufficient data that both hyperperfused rim and reversibly electroporated periphery of IRE lesion coincide in the exactly same place.

Our results clearly demonstrate that combination treatment using IRE followed by DEB-TACE with doxorubicin achieves complementary therapeutic effects.

Vollherbst et al. compared the use of chemoembolization (lipiodol, doxorubicin and 100 μm beads) followed by IRE, IRE followed by chemoembolization, and IRE alone [11]. No difference concerning the size of the ablation zone between the groups was seen, which could be explained by the rather small group size of two animals per group, the

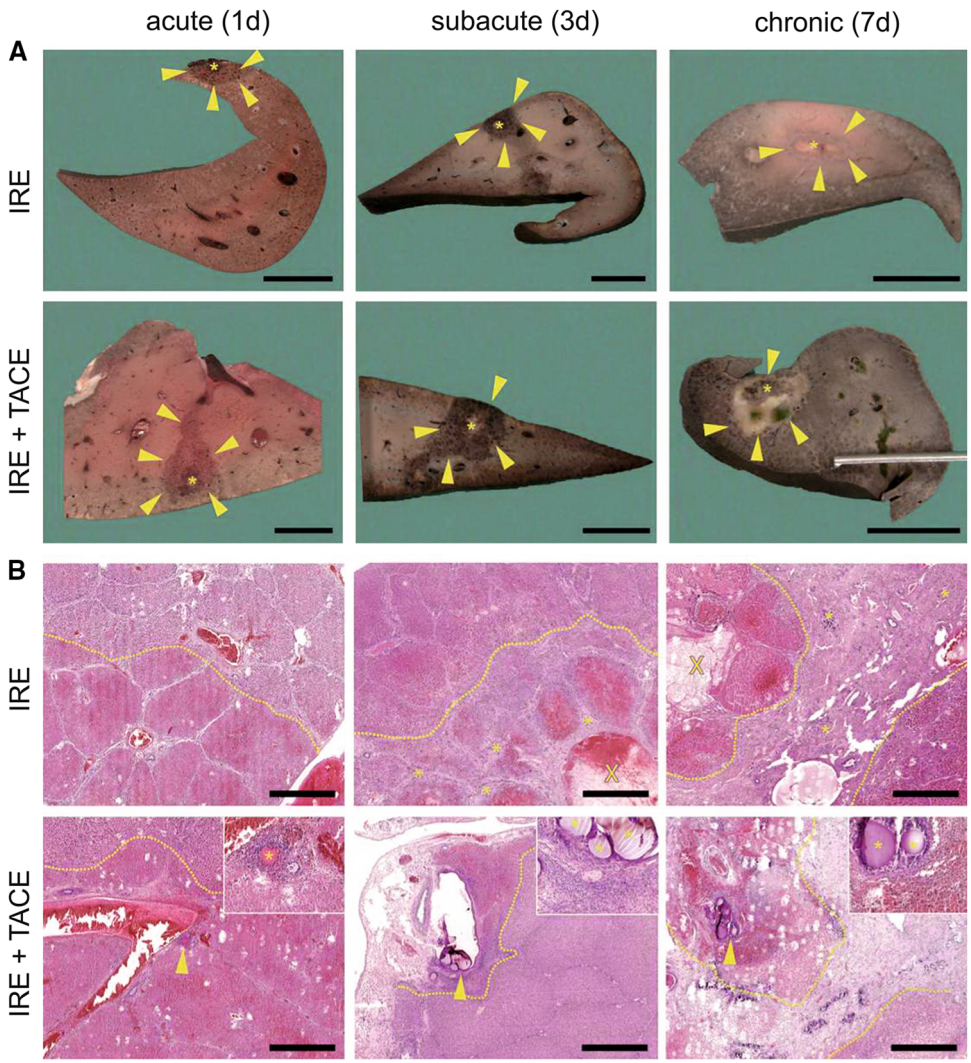

Fig. 3 Macroscopic (**A**) and microscopic (**B**) photographs of liver specimens after necropsy of animals after IRE or IRE + TACE after acute (1 day follow-up), subacute (3 days of follow-up) and chronic (7 days of follow-up). **A** Asterisks mark necrotic areas; arrowheads mark hemorrhagic rim that is transformed into a zone of fibrosis in the chronic group (reference bar: 2 cm). **B** Dotted line marks border between necrosis (above line) and hemorrhagic rim (below line) in acute and subacute groups. In chronic group, zone of fibrosis demarcates between necrosis (above line on the top left) and regular liver tissue (below line on the lower right). Asterisks mark hemorrhagic infiltrations in acute and subacute groups and fibrosis in the chronic group. Arrowheads mark DEB particles in arterial vessels

short follow-up of only 2 h or the different technique of chemoembolization.

Although doxorubicin distribution was not analyzed directly, the distribution of the beads—acting as a surrogate—was assessed. In slices containing IRE + DEB-TACE lesions, the majority of beads (69%) were detected inside the hemorrhagic infiltration surrounding the ablation volumes, emphasizing the accumulating effect of hyperperfusion induced by the IRE preceding the TACE. The remaining 31% of beads were found inside the ablation volumes, reflecting the sustained perfusion of the tissue during and after IRE.

Both IRE and IRE + DEB-TACE lesions shrank in size during the 7 days of follow-up. This effect is also observed in clinical IRE, where lesions including the treated tumor vanish during follow-up and are replaced by regular liver tissue [12–14]. Probably this effect is accelerated in our experiments, since healthy liver tissue and no tumor were treated. The profound shrinkage of the ablation lesions naturally leads to a decrease in differences between lesion volumes of the IRE and the IRE + DEB-TACE group, rendering the difference at day 7 not statistically different.

The following limitations apply to our study.

The size of the experimental group is limited to nine animals due to the animal experiment regulatory board allowance. We did not directly analyze intracellular deposition of doxorubicin, but investigated the distribution of DEB in the tissue serving a surrogate for doxorubicin deposition.

Furthermore, we did not use a tumor model, since tumor models are only available in small animals. We intended to investigate the additional value of TACE after IRE. In clinical application, local perfusion after IRE is mainly determined by ablation effects, since the tumor is already treated. In this context, the additional value of a tumor model was weighed against good comparability with the use of the clinical IRE system and was determined to be of less importance. Therefore, further clinical investigations

have to determine whether IRE immediately followed by DEB-TACE yields a superior oncologic outcome.

Ablation volume measurements are based on CT imaging and not on pathological analysis. Our choice allows us to use more data (nine and six animals in acute/subacute groups), and due to the fact that the portal venous contrast phase was used, we assume that possible arterial occlusion by DC-Beads has no influence on the ablation measurements.

Not lesion diameters but lesion volume was assessed in this study. Therefore, information about sphericity cannot be given.

Due to a limitation of group size (due to limitations of the animal experiment allowance), we did not investigate the role of different therapy sequences, i.e., if first IRE, thereafter ablation or vice versa leads to the optimal ablative result.

Due to the study setup using two applicators instead of 3–6 applicators, lesion sizes are in total comparably small. Therefore, standard deviation of lesion volumes is comparably high.

In conclusion, the sequential combination of IRE followed by DEB-TACE loaded with doxorubicin resulted in a selective accumulation of beads leading to significantly larger ablation zone when compared to IRE alone, allowing a more aggressive treatment, which could especially be helpful for the treatment of large tumors. Further studies need to evaluate safety and efficacy of the combination treatment in the clinical setting.

Compliance with Ethical Standards

Conflict of interest The authors declare that they have no conflict of interest.

Ethical Approval All applicable international, national, and/or institutional guidelines for the care and use of animals were followed.

Informed Consent For this type of study, informed consent is not required.

Consent for Publication For this type of study, consent for publication is not required.

References

1. Bower M, Sherwood L, Li Y, Martin R. Irreversible electroporation of the pancreas: definitive local therapy without systemic effects. J Surg Oncol. 2011;104(1):22–8.
2. Perera M, Krishnananthan N, Lindner U, Lawrentschuk N. An update on focal therapy for prostate cancer. Nat Rev Urol. 2016;13(11):641–53.
3. Niessen C, Igl J, Pregler B, et al. Factors associated with short-term local recurrence of liver cancer after percutaneous ablation using irreversible electroporation: a prospective single-center study. J Vasc Interv Radiol. 2015;26(5):694–702.
4. Dollinger M, Jung EM, Beyer L, et al. Irreversible electroporation ablation of malignant hepatic tumors: subacute and follow-up CT appearance of ablation zones. J Vasc Interv Radiol. 2014;25(10):1589–94.
5. Chung DJ, Sung K, Osuagwu FC, Wu HH, Lassman C, Lu DS. Contrast enhancement patterns after irreversible electroporation: experimental study of CT perfusion correlated to histopathology in normal porcine liver. J Vasc Interv Radiol. 2016;27(1):104–11.
6. Davalos RV, Mir IL, Rubinsky B. Tissue ablation with irreversible electroporation. Ann Biomed Eng. 2005;33(2):223–31.
7. Kotnik T, Frey W, Sack M, Haberl Meglic S, Peterka M, Miklavcic D. Electroporation-based applications in biotechnology. Trends Biotechnol. 2015;33(8):480–8.
8. Lammer J, Malagari K, Vogl T, et al. Prospective randomized study of doxorubicin-eluting-bead embolization in the treatment of hepatocellular carcinoma: results of the PRECISION V study. Cardiovasc Intervent Radiol. 2010;33(1):41–52.
9. Ni JY, Liu SS, Xu LF, Sun HL, Chen YT. Transarterial chemoembolization combined with percutaneous radiofrequency ablation versus TACE and PRFA monotherapy in the treatment for hepatocellular carcinoma: a meta-analysis. J Cancer Res Clin Oncol. 2013;139(4):653–9.
10. Dev SBRD, Widera G, Hofmann GA. Medical applications of electroporation. IEEE Trans Plasma Sci. 2000;28(1):206–23.
11. Vollherbst D, Bertheau RC, Fritz S, et al. Electrochemical effects after transarterial chemoembolization in combination with percutaneous irreversible electroporation: observations in an acute porcine liver model. J Vasc Interv Radiol. 2016;27(6):913–21.
12. Lee EW, Chen C, Prieto VE, Dry SM, Loh CT, Kee ST. Advanced hepatic ablation technique for creating complete cell death: irreversible electroporation. Radiology. 2010;255(2):426–33.
13. Lee EW, Wong D, Tafti BA, et al. Irreversible electroporation in eradication of rabbit VX2 liver tumor. J Vasc Interv Radiol. 2012;23(6):833–40.
14. Appelbaum L, Ben-David E, Sosna J, Nissenbaum Y, Goldberg SN. US findings after irreversible electroporation ablation: radiologic-pathologic correlation. Radiology. 2012;262(1):117–25.